


RESEARCH ARTICLE

Poacic acid, a β -1,3-glucan-binding antifungal agent, inhibits cell-wall remodeling and activates transcriptional responses regulated by the cell-wall integrity and high-osmolarity glycerol pathways in yeast

Raúl García¹ | Kaori Itto-Nakama² | José Manuel Rodríguez-Peña¹ | Xiaolin Chen² | Ana Belén Sanz¹ | Alba de Lorenzo¹ | Mónica Pavón-Vergés¹ | Karen Kubo² | Shinsuke Ohnuki² | César Nombela¹ | Laura Popolo³ | Yoshikazu Ohya^{2,4} | Javier Arroyo¹ 

¹Departamento de Microbiología y Parasitología, Facultad de Farmacia, Universidad Complutense de Madrid, IRYCIS, Madrid, Spain

²Department of Integrated Biosciences, Graduate School of Frontier Sciences, University of Tokyo, Kashiwa, Japan

³Department of Biosciences, University of Milan, Milan, Italy

⁴Collaborative Research Institute for Innovative Microbiology (CRIIM), The University of Tokyo, Tokyo, Japan

Correspondence

Yoshikazu Ohya, Department of Integrated Biosciences, Graduate School of Frontier Sciences, University of Tokyo, Kashiwa, Chiba, Japan.
Email: ohya@edu.k.u-tokyo.ac.jp

Javier Arroyo, Departamento de Microbiología y Parasitología, Facultad de Farmacia, Universidad Complutense de Madrid, IRYCIS, 28040 Madrid, Spain.
Email: jarroyo@ucm.es

Funding information

This work was supported by grants BIO2016-79289-P and PID2019-105223GB-I00 (Ministerio de Ciencia e Innovación, MICINN, Spain) and S2017/BMD3691-InGEMICS (Comunidad de Madrid, Spain) to J.A. “Center of excellence for Glycomics”, ITMS 26240120031 (Research & Development

Abstract

As a result of the relatively few available antifungals and the increasing frequency of resistance to them, the development of novel antifungals is increasingly important. The plant natural product poacic acid (PA) inhibits β -1,3-glucan synthesis in *Saccharomyces cerevisiae* and has antifungal activity against a wide range of plant pathogens. However, the mode of action of PA is unclear. Here, we reveal that PA specifically binds to β -1,3-glucan, its affinity for which is ~30-fold that for chitin. Besides its effect on β -1,3-glucan synthase activity, PA inhibited the yeast glucan-elongating activity of Gas1 and Gas2 and the chitin-glucan transglycosylase activity of Crh1. Regarding the cellular response to PA, transcriptional co-regulation was mediated by parallel activation of the cell-wall integrity (CWI) and high-osmolarity glycerol signaling pathways. Despite targeting β -1,3-glucan remodeling, the transcriptional profiles and regulatory circuits activated by caspofungin, zymolyase, and PA differed, indicating that their effects on CWI have different mechanisms. The

Abbreviations: AB, aniline blue; BGT, β -1,3-glucanosyltransferase; CA, caffeic acid; CM, carboxymethyl; CRH, Congo red-hypersensitive; CW, calcofluor white; CWI, cell-wall integrity; FA, ferulic acid; FDR, false discovery rate; HOG, high-osmolarity glycerol; MAPK, mitogen activated protein kinase; PA, poacic acid; PKA, protein kinase A; RNA-seq, RNA-sequencing; SD, synthetic dextrose; SR, sulphorhodamine; VIF, variance inflation factor; WT, wild-type; YPD, yeast extract peptone dextrose.

Raúl García, Kaori Itto-Nakama and José Manuel Rodríguez-Peña contributed equally to this work.

This is an open access article under the terms of the Creative Commons Attribution-NonCommercial License, which permits use, distribution and reproduction in any medium, provided the original work is properly cited and is not used for commercial purposes.

© 2021 The Authors. *The FASEB Journal* published by Wiley Periodicals LLC on behalf of Federation of American Societies for Experimental Biology

Operational Programme funded by the ERDF) to Vladimír Farkaš, and 19H03205 and 18K14351 (Grants-in-Aid for Scientific Research from the Ministry of Education Culture, Sports, Science and Technology, Japan) to Y.O and K.I.N, respectively

effects of PA on the growth of yeast strains indicated that it has a mode of action distinct from that of echinocandins, suggesting it is a unique antifungal agent.

KEYWORDS

β -1,3-glucan, antifungal agents, cell wall remodeling, MAPK, poacic acid, *Saccharomyces cerevisiae*, transcriptomics, transglycosylases

1 | INTRODUCTION

Human invasive fungal infections have mortality rates exceeding 50% despite the availability of several effective antifungals,¹ a situation exacerbated by antifungal resistance.² Given the limited arsenal of available antifungal agents and the frequency of resistance, the search for antifungal drugs with new modes of action is crucial. The importance of the cell wall for fungal viability, together with the absence in mammals of the components and enzymes necessary for cell-wall biogenesis and remodeling, make this structure an attractive target for therapeutic intervention against fungal infections.^{3–5}

The yeast cell wall is composed of an inner layer comprising the polysaccharides β -1,3-glucan, β -1,6-glucan, and chitin, and an outer layer of mannoproteins.^{6,7} These components are synthesized and connected in a precise order that guarantees functionality. The network backbone is formed by β -1,3-glucan, the most abundant cell wall component, which creates a branched mesh surrounding the cell surface, to which β -1,6-glucan and chitin are attached.⁸ Although the fungal cell wall appears to be rigid, it is a highly dynamic structure. It is remodeled during cell growth by elongation, branching, and cross-linking of newly synthesized polysaccharides, the extant cell-wall matrix. Much progress has been made in the functional characterization of the fungal enzymes involved in these processes. The Gas1/Gel1/Phr1 family of β -1,3-glucanases mediates the elongation and branching of β -1,3-glucan, acting as β -1,3-glucanosyl transferases.^{9–11} Additionally, the conserved Congo red-hypersensitive (CRH) family of fungal cell-wall transglycosylases is responsible for the formation of cross-links between chitin and glucan (β -1,6 or β -1,3).^{12–15}

Cell-wall remodeling is essential for counteracting stress conditions that weaken cell-wall integrity (CWI). Consequently, cell-wall perturbing agents induce rescue responses, which involve compensatory synthesis of cell-wall materials and alteration of the cross-linking between cell-wall polymers necessary to maintain fungal integrity.^{16,17} Many of these changes result from transcriptional reprogramming that involves the induction of a large group of genes related to cell-wall biogenesis.^{18–20} The yeast CWI pathway, governed by the mitogen-activated protein kinase (MAPK) Slt2, is the key signaling cascade that regulates cell-wall

stress responses, but other pathways are also implicated.^{16,20} Stress at the cell surface is detected by five putative plasma membrane mechanosensors, grouped into two types, namely, (i) Wsc1 to Wsc3 and (ii) Mid2 and Mtl1.²¹ These sensors transduce the signal to the GDP/GTP exchange factor Rom2, activating the small GTPase Rho1. GTP-bound Rho1 interacts with and activates Pkc1, triggering the MAPK cascade.²² Phosphorylation of the MAPKKK Bck1 activates a pair of redundant MAPKKs (Mkk1 and Mkk2), which phosphorylate Slt2. The phosphorylated form of this protein acts mainly on two transcription factors, Rlm1 and SBF (Swi4/6) (see^{16,23} and references therein). Rlm1 activates the expression of the majority of cell-wall stress-response genes,^{20,24} including *CRH1*,²⁵ the most relevant member of the CRH family. These findings suggest the importance of cell wall cross-linking to survival under stress conditions that impair cell wall.

Subtle differences in the regulatory mechanisms controlling the transcriptional response to cell-wall stress have been described. Binding of Congo red to chitin is sensed by Mid2 and elicits a transcriptional response that relies almost entirely on the MAPK Slt2 and the transcription factor Rlm1.^{18,26} Cell-wall damage caused by zymolyase, which degrades the β -1,3-glucan network, induces sequential activation of the high-osmolarity glycerol (HOG) and CWI pathways. A considerable portion of the transcriptional response under these conditions is dependent on Slt2 and Rlm1, but the activation of Slt2 depends on Hkr1 and components of the Sho1 branch of the HOG pathway.^{27–29} Another type of CWI/HOG co-regulation of cell-wall-related genes has been reported for ethanol stress.³⁰ Inhibition of β -1,3-glucan synthesis by echinocandins induces activation of the CWI pathway via Wsc1, resulting in induction of Rlm1-dependent genes and parallel inhibition of the protein kinase A (PKA) pathway. The result is induction of the transcription of several genes independently of Slt2.^{31,32}

To date, the development of novel cell-wall-targeted antifungals has focused on inhibiting the synthesis of cell-wall components. The echinocandins caspofungin, micafungin, and anidulafungin, the newest antifungal agents on the market, bind to and inhibit β -1,3-D-glucan synthase (reviewed in^{33–35}). Other drugs under development also target the synthesis of β -1,3-glucan, chitin, or glycosylphosphatidylinositol and the consequent attachment of essential glycosylphosphatidylinositol-linked proteins to the outer

cell wall.³ Poacic acid (diferulate, 8–5-DC; PA) was identified as a novel natural antifungal agent by screening a collection of diferulates found in lignocellulosic hydrolysates using *Saccharomyces cerevisiae* as a discovery platform.³⁶ The postulated cellular target for PA is the β -1,3-glucan cell wall network. The interaction of PA with the cell wall leads to growth inhibition of several fungal species, such as the phytopathogenic fungi *Sclerotinia sclerotiorum* and *Alternaria solani*, as well as *S. cerevisiae*.³⁶ PA showed a species-dependent effect on the genus *Candida*.³⁷ Genomic–phenotypic studies implicated several factors in PA sensitivity, including the CWI pathway and interacting genes.³⁶ PA inhibits β -1,3-glucan synthesis, but unlike the echinocandins it directly binds to the glucan network rather than inhibiting glucan synthase.^{36,37} It has been suggested that direct binding of PA to β -1,3-glucan interferes with polysaccharide maturation, leading to a weaker cell wall, but the mechanism of action is unknown. It is also uncertain whether PA can bind to other cell-wall components or polysaccharides because only qualitative evidence was provided.³⁶

We evaluated the mechanism underlying the effect of PA on β -1,3-glucan network integrity. We first identified the primary binding target polymer of PA in the cell wall to clarify the structural motif required. We further demonstrated that PA inhibits the activity of Gas and Crh cell-wall-remodeling enzymes. Furthermore, we analyzed the global transcriptional pattern elicited in yeast by PA and its regulation. Notably, we demonstrated that the PA adaptive response follows a regulatory pattern not previously reported for other cell-wall-interfering agents. Finally, we explored the effect of PA on the growth of several yeast strains. Taken together, our findings indicate that PA has a mode of action distinct from that of echinocandins and has potential as an antifungal agent.

2 | MATERIALS AND METHODS

2.1 | Yeast strains

The yeast strains used in this study are listed in Table S1.

2.2 | Growth conditions

Yeast cells were routinely cultured overnight in yeast extract peptone dextrose (YPD) medium (2% glucose, 2% peptone, and 1% yeast extract) at 220 rpm and 24°C to an absorbance at 600 nm (A_{600}) of 0.8–1. The culture was refreshed to an A_{600} of 0.2 using YPD, incubated for 2 hour and divided into two parts. One part was allowed to continue growing under the same conditions (nontreated culture), and the other was supplemented with PA (a gift from Fachuang Lu, Ruili Gao, Jeff

Piotrowski, and John Ralph at The University of Wisconsin) to a final concentration of 100 μ g/mL. The cells were collected and subsequently processed according to the experimental approach.

For metachromatic interaction and PA susceptibility experiments, *S. cerevisiae* and *Candida albicans* were first cultured on YPD agar (1% yeast extract [BD Biosciences, San Jose, CA], 2% polypeptone [Fujifilm Wako Pure Chemical Corporation, Osaka, Japan], 2% glucose [Fujifilm Wako Pure Chemical Corporation, Osaka, Japan] and 2% agar [Fujifilm Wako Pure Chemical Corporation, Osaka, Japan]). Single colonies were inoculated into rich medium YPD or synthetic dextrose (SD; 0.67% yeast nitrogen base without amino acids [BD Biosciences] and 2% glucose) growth medium supplemented appropriately and incubated at 30 or 25°C with shaking at 200 rpm. For Ura or Leu selection, 0.5% casamino acids (BD Biosciences) was added to SD medium.

2.3 | Metachromatic interaction

A quartz cuvette containing 0.1 mL of a 15 μ g/mL solution of PA, ferulic acid (FA; LKT Labs, MN), or caffeic acid (CA; Tokyo Chemical Industry Co., Ltd., Tokyo, Japan) was scanned spectrophotometrically from 260 to 460 nm using an ultraviolet/visible spectrophotometer (Amersham Biosciences Ultrospec 2100pro), and the sample absorbance was continuously recorded. β -1,3-glucan (laminarin [Tokyo Chemical Industry Co., Ltd., Tokyo, Japan]), β -1,6-glucan (pustulan [Carbosynth Co., Ltd., United Kingdom]), chitin (Tokyo Chemical Industry Co., Ltd., Tokyo, Japan), and cellulose (Sigma-Aldrich, St. Louis, MO) were added to a cuvette containing the dye and repeatedly scanned spectrophotometrically. An interaction between polymer and dye was indicated by a shift in the maximum absorbance value.

2.4 | Staining of cell-wall components

Yeast cells were cultured overnight in YPD, collected, washed once with phosphate-buffered saline pH 7.4, and harvested again by centrifugation. The cells were stained with 50 μ g/mL PA, 0.5 mg/mL aniline blue (AB) (Fujifilm Wako Pure Chemical Corporation, Osaka, Japan), or 1 mg/mL calcofluor white (CW) (Sigma Aldrich, St. Louis, MO). CW-stained cells were washed twice with 1 mL of distilled water to eliminate unbound dye. Stained cells were observed under a fluorescence microscope (Axio Imager with a 6100 ECplan-Neofluar lens [Carl Zeiss, Oberkochen, Germany] and a CoolSNAP HQ cooled charge-coupled-device camera [Roper Scientific Photometrics, Tucson,

AZJ], and AxioVision software (Carl Zeiss). An AB filter was used to visualize PA- and AB-stained cells (Carl Zeiss; 359–371 nm excitation, 515–565 nm emission) and a 4',6-diamidino-2-phenylindole filter for CW-stained cells (Carl Zeiss; 358 nm excitation, 461 nm emission). Images were analyzed using ImageJ (ver. 1.49). TIFF files were created using a threshold to maintain the fluorescence signal in an appropriate range.

2.5 | Statistical analysis

Because the fluorescence signal intensity is proportional to the cell-wall polysaccharide content, a linear model was constructed based on the data obtained to statistically analyze the affinity of PA for the polysaccharides. The linear model is:

$$I_i^{\text{PA}} = \beta_0 + \beta_1 I_i^{\text{AB}} + \beta_2 I_i^{\text{CW}} + \varepsilon_i$$

$$\varepsilon_i \sim N(a, b)$$

where I_i^{PA} : Intensity of fluorescent signal of PA, which binds to β -1,3-glucon and chitin; I_i^{AB} : Intensity of fluorescent signal of aniline blue, which binds to β -1,3-glucon; I_i^{CW} : Intensity of fluorescent signal of calcofluor, which binds to chitin.

The linear predictor contains three unknown parameters to be estimated from the data. The errors follow a gamma distribution, and identity link ($\eta(y) = y$) was used as the link function. Statistical analysis was performed using R software (<http://www.rproject.org>).

2.5.1 | Likelihood-ratio test

To examine the fit of the data set to the model, the likelihood-ratio test was used with a linear model. The likelihood formula is: $\text{LR} = 2(\ln L_1 - \ln L_2)$, in which L_1 and L_2 are the maximum-likelihood score of the complicated model. LR follows a chi-squared distribution, and the degree of freedom is the difference value of several parameters in two models. On this basis, and according to the table of χ^2 values versus P -values, we determined the model's goodness of fit.

2.5.2 | Collinearity

The collinearity of the predictor variables in the multiple regression model was evaluated by calculating the variance inflation factor (VIF). A regression of x_i on all other predictors gives R_i^2 and the VIF, a measure of multicollinearity, is defined as: $\text{VIF} = 1/(1-R_i^2)$. A rule of thumb is that a VIF of >5 indicates high multicollinearity.

2.6 | RNA-sequencing (RNA-seq)

To generate NGS libraries, ribosomal RNA was depleted from total RNA samples by hybridization with specific probes. A Ribo-Zero Gold Yeast Kit (Illumina) was used with 5 μg of total RNA, following the manufacturer's instructions. Total RNA isolation and purification were carried out as described previously.¹⁸

DNA libraries were generated from depleted RNA using a NEBNext Ultradirectional RNA Library Prep Kit (New England Biolabs) following the manufacturer's instructions. Briefly, depleted RNA was fragmented and copied to double-stranded cDNA. Specific adapters for Illumina sequencing were attached to the cDNAs and the library was enriched by limited PCR. DNA fragments with inserts of 300–450 bp were subjected to massively parallel sequencing at the Genomics Unit (UCM).

RNA-seq data were analyzed using CLC Genomics Workbench (Qiagen Bioinformatics) to identify differentially expressed genes. Clean reads were obtained by trimming low-quality reads, and the high-quality reads were aligned to the *S. cerevisiae* genome (R64-1-1) using the default parameters. Expression values were measured in reads per kilobase of exon model per million mapped reads (RPKM). The threshold P -value was determined according to the false discovery rate (FDR). In this study, genes that met the following criteria were considered differentially expressed: FDR P -value $\leq .05$ and fold change ≥ 2 for upregulated or ≤ 0.5 for downregulated genes. To determine whether the gene induction observed in the wild-type (WT) strain after PA treatment (100 $\mu\text{g}/\text{mL}$, 1 hour) was significantly reduced in the *slt2* Δ mutant, we compared the response of the mutant (mutant ratio) to that of the WT (WT ratio). A mutant ratio \div WT ratio value of 0.65 was considered the threshold for a significant reduction in gene expression.²⁸ Genes that exhibited an expression ratio in the mutant of <1.65 were not deemed to be upregulated. To analyze the alternative response in the *slt2* Δ strain, we considered those genes that were induced at least twofold in this mutant and, in turn, at least 1.5 fold with respect to the WT strain.

For RNA-seq, each group contained three library samples. We used the differential expression for RNA-Seq tool in CLC Genomics Workbench to perform multi-factorial statistical analysis on a set of expression tracks based on a negative binomial generalized linear model.

2.7 | Quantitative real-time PCR

Quantitative RT-PCR (RT-qPCR) was performed as described.¹⁸ To quantify gene expression, the transcript abundance was determined relative to that of *ACT1* for input cDNA normalization, and the relative gene expression levels

of treated versus nontreated samples were calculated by the $2^{-\Delta\Delta Ct}$ method.³⁸ Primer sequences are available upon request.

2.8 | Western blotting

Western blotting—including cell collection and lysis, fractionation of proteins by sodium dodecyl sulfate-polyacrylamide gel electrophoresis, and transfer of proteins to nitrocellulose membrane—was carried out as described.²⁷

2.9 | Gas and Crh activity assays

The β -1,3-glucanotransferase (BGT) activity of Gas1 and Gas2 was assayed as described previously.¹⁰ The assay mixture contained 40 μ M sulphorhodamine (SR)-labeled laminaripentaose (L5-SR), 2.5 mg/mL laminarin, 1.2 or 0.6 μ g of purified Gas1 and Gas2 recombinant proteins and 250 mM citrate-phosphate buffer (pH 5 or 6), in a total volume of 20 μ L.

The transglycosylase activity of Crh1 was measured as described previously³⁹ with slight modifications. In this case, the incubation mixture contained 0.1% carboxymethyl (CM)-chitin, 18 μ M SR-labeled oligosaccharides (L5-SR or SR-labelled chitopentaose [CH5-SR]), 0.5 μ g of Crh1 protein and 50 mM citrate buffer (pH 4.9) in a total volume of 20 μ L.

In the two enzymatic assays, the corresponding concentration of PA (0, 150 or 300 μ g/mL) was added to the reaction mixture before adding the enzyme and incubated at 37°C for 10-90 minutes. Enzymatic activity was measured by quantifying fluorescence intensity using a FluoStar Omega Reader (BMH Labtech).

2.10 | PA susceptibility of WT and *fks1-ts* mutant *S. cerevisiae* strains

Cells of WT yeast strains⁴⁰ and *fks1-ts* mutants⁴¹ were grown in YPD at 25°C with shaking at 200 rpm to logarithmic phase (1×10^7 cells/mL). The cultures were diluted with fresh YPD to 5×10^4 cells/mL and mixed with PA (15.6, 31.3, 62.5, 125, 250, 500, 1000 μ g/mL) or echinocandin B (3.1, 6.3, 13, 25, 50, 100, 150 μ g/mL) in 96-well microtiter plates. After incubation for 24 hours at 25°C, the cell suspension was stirred by pipetting, and growth was evaluated by measuring the A_{600} using a Spectra Max Plus 384 Plate Reader (Molecular Devices). The PA concentrations resulting in 10% and 50% inhibition (IC_{90} and IC_{50}) were calculated from dose-response curves using the four-parameter logistic function in R. To analyze the correlation between the β -1,3-glucan content

and PA IC_{50} values of *S. cerevisiae* strains, we calculated Pearson's product-moment correlation using R software.

3 | RESULTS

3.1 | Metachromatic interaction between PA and β -1,3-glucan

To investigate in vitro the interaction between PA and cell-wall polymers, we observed metachromasia. Upon binding of PA to polymers, its color may change as a result of metachromatic dye-polymer interactions, leading to a shift in the spectrum absorption peak. We examined the spectrum of PA (15 μ g/mL) in the presence and absence of β -1,3-glucan, and observed a distinct red-shift in the absorption peak from 318 nm for free PA to 327 nm for β -1,3-glucan-bound PA (Figure 1A). This 9 nm red-shift suggested a metachromatic interaction between PA and β -1,3-glucan. By contrast, the PA absorption peak did not change notably in the presence of β -1,6-glucan, chitin, or cellulose (Figure 1B-D), implying that PA interacts preferentially with β -1,3-glucan.

PA is synthesized by coupling reactions of phenolic acids, such as FA. We next examined the interaction of FA and another phenolic acid, CA, with cell-wall polymers (Figure S1). FA (15 μ g/mL) and CA (15 μ g/mL) showed no red-shift but a distinct blue-shift (4-5 nm) in the presence of β -1,3-glucan (Figure S1Ba,Ca). In contrast, the absorption peaks of FA and CA did not change notably in the presence of β -1,6-glucan, chitin, or cellulose (Figure S1Bb-d,Cb-d), supporting the specificity of the interactions between these phenolic acids and β -1,3-glucan.

Metachromasia is dependent on the dye concentration. We examined the dose-dependency of the absorption-peak shift of PA, FA, and CA in the presence of β -1,3-glucan. Concentration-dependent shift of PA was observed up to 15 μ g/mL (Figure S1D), being the shift longer for PA than for FA and CA (Figure S1D). Of the three compounds, only PA showed the inhibition of yeast cell growth (Figure S1E), suggesting a correlation between the binding of PA to β -1,3-glucan and yeast cell growth inhibition.

3.2 | Binding affinity of PA to β -1,3-glucan and chitin of yeast cells

Visualization of cell wall components β -1,3-glucan and chitin can be achieved by staining yeast cells with fluorescent dyes AB and CW, respectively.⁴² AB interacts preferentially with β -1,3-glucans,^{43,44} whereas CW behaves as a specific chitin dye.^{45,46} Thus, CW fluorescence intensity in yeast cells has been found to be an accurate reflection of the relative chitin content.^{45,47} Methods using AB fluorescence assays have also

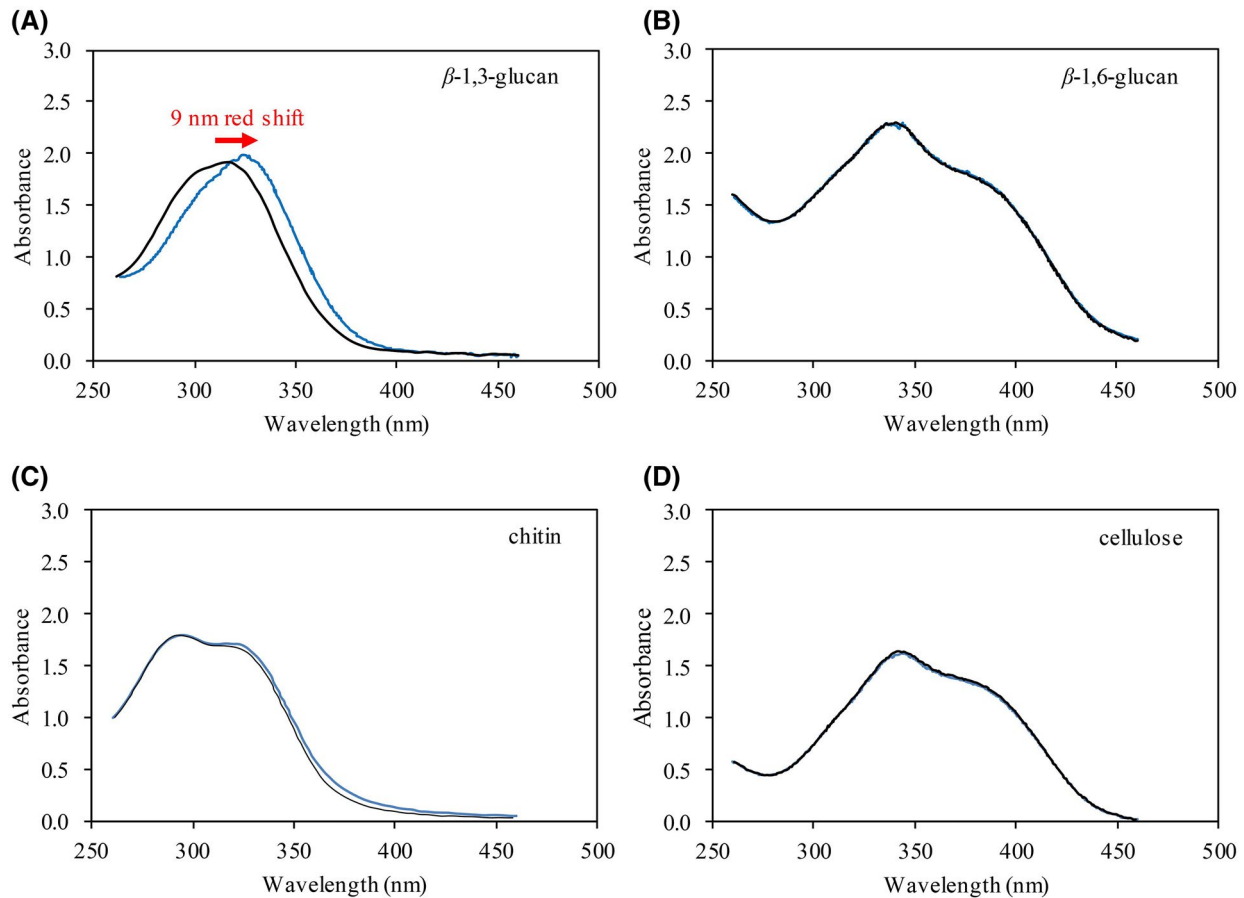


FIGURE 1 Metachromatic interaction between poaic acid (PA) and cell-wall components. Metachromatic interaction between PA (15 $\mu\text{g mL}$) and β -1,3-glucan (A), β -1,6-glucan (B), cellulose (C), and chitin (D). Spectra of PA with (blue) and without polymers (black) are shown. The red-shift of the absorption peak was observed from 318 nm for free PA to 327 nm for β -1,3-glucan-bound PA (red). Experiments were repeated three times and yielded similar results

been widely used to quantify fungal β -1,3-glucans.^{37,48–50} In a previous study, direct binding of PA to β -1,3-glucan was only qualitatively evaluated using a dye-binding assay.³⁶ We extended this analysis by examining the binding activity of PA to β -1,3-glucan and chitin with combinatory use of AB and CW.

The PA fluorescence signal intensity is proportional to the level of target polysaccharide. Therefore, the signal intensity of PA (I_i^{PA}) in yeast strains was subjected to multiple regression analysis using the signal intensities of β -1,3-glucan (I_i^{PA}) and chitin (I_i^{CW}) as predictor variables. The linear model was constructed as follows:

$$I_i^{\text{PA}} = \beta_0 + \beta_1 I_i^{\text{AB}} + \beta_2 I_i^{\text{CW}} + \varepsilon_i$$

The linear predictor contained one constant term (β_0) and two regression coefficients (β_1 and β_2) to be estimated from the data. The errors followed a gamma distribution, and identity link ($\eta(y) = y$) was used as the link function. Examination of six yeast strains with different β -1,3-glucan and chitin contents (Figure S2A–C) yielded the following linear formula:

$$I_i^{\text{PA}} = 240.7 + 0.1765 I_i^{\text{AB}} + 0.005717 I_i^{\text{CW}} + \varepsilon_i$$

Because β_1 and β_2 were 0.1765 and 0.005717, respectively, β_1/β_2 was calculated to be 30.87, and so the affinity of PA for β -1,3-glucan is \sim 30-fold that of chitin.

To test the goodness of fit, we performed a likelihood-ratio test. Analysis of the linear predictor and actual intensity data yielded an R^2 of 0.773, indicating significant goodness of fit ($P < .0001$, likelihood-ratio test) (Figure S2D). We also tested the collinearity of the predictor variables in the multiple regression model by calculating VIF. The regression coefficients for that term are appropriately estimated if the VIF is < 5 . The VIF was 2.162, suggesting negligible multicollinearity. Therefore, the primary target of PA is β -1,3-glucan in yeast cells.

3.3 | PA inhibits β -1,3-glucan cell-wall remodeling mediated by Gas and Crh transglycosylases

PA binds β -1,3-glucan and thereby inhibits glucan synthesis mediated by the β -1,3-glucan synthase.³⁶ To test the possibility that PA also interferes with β -1,3-glucan maturation, we

assayed the glucanosyltransferase activity of purified Gas1 and Gas2 enzymes in the absence or presence of PA. For this purpose, we used laminarin as the donor substrate and sulforhodamine (SR)-labelled laminarioligosaccharides of five glucose residues (L5-SR) as acceptors and measured the formation of fluorescent hybrid polymer molecules after the addition of the enzyme. As shown in Figure 2, PA partially inhibited the activity of both enzymes in a dose-dependent manner.

β -1,3-Glucan becomes crosslinked to chitin via members of the conserved CRH family, generating covalent links between the reducing ends of chitin chains and the non-reducing ends of β -1,6- and β -1,3-glucan chains.^{8,13,14} Therefore, we assayed the activity of purified Crh1 using soluble CM-chitin as the donor and the fluorescent SR-labelled oligosaccharides derived from β -1,3-glucan (L5-SR) as acceptors in the presence and absence of PA. PA inhibited Crh1 activity under these conditions in a dose-dependent manner (Figure 2). In addition to their function as chitin–glucan transglycosylases,

Crh proteins act as homotransglycosylases, joining and elongating nascent chitin chains.³⁹ However, we found no significant inhibition of Crh1-mediated TG activity by PA when the acceptors used in the reaction were oligosaccharides derived from chitin (CH5-SR) instead of oligosaccharides derived from β -1,3-glucan (Figure 2), in agreement with the hypothesis that binding of PA to β -1,3-glucan interferes with the maturation of this polymer. Thus, PA would bind β -1,3-glucan interfering with the transglycosylation processes required for β -1,3-glucan maturation and proper remodeling of the yeast cell wall.

3.4 | PA induces transient but lasting activation of the CWI pathway and activates a transcriptional response to cell-wall stress

The MAPK Slt2 was activated in a WT strain after 10 minutes of exposure to high concentrations of PA.³⁷ We next

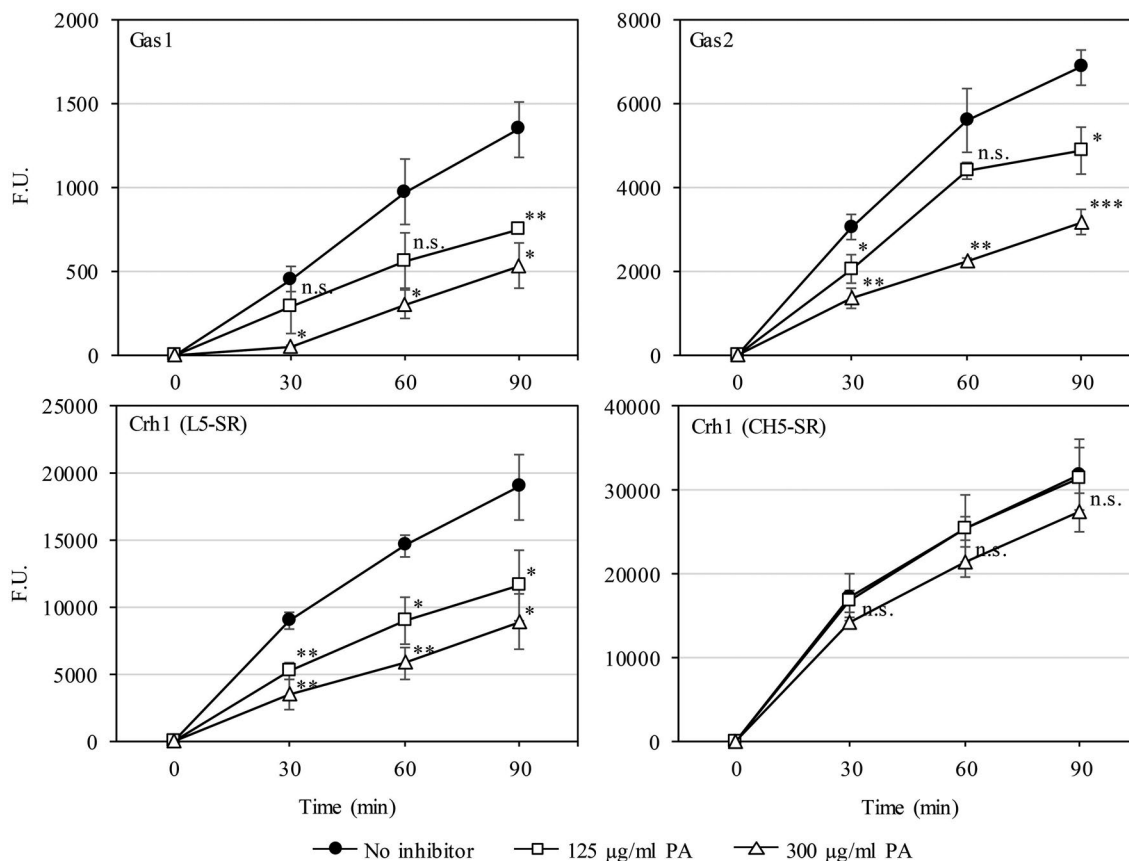


FIGURE 2 Effects of poacic acid (PA) on the transglycosylase activity of Gas and Crh proteins. Upper panel, β -1,3-Glucanosyltransferase activity of Gas1 and Gas2 proteins at the indicated times in the absence (no inhibitor) or presence of 125 or 300 μ g/mL PA. The 20- μ L assay mixture contained 1.2 μ g of Gas1 or 0.6 μ g of Gas2 protein, 40 μ M SR-labeled laminarioligopentaose (L5-SR) as the acceptor, and laminarin (2.5 mg mL) as the donor in 50 mM citrate-phosphate buffer, pH 5 (Gas1) or pH 6 (Gas2). Lower panel, Crh1 transglycosylase activity of Crh1 at the indicated times in the absence (no inhibitor) or presence of 125 or 300 μ g/mL PA. The 20- μ L transglycosylation assay mixture contained 0.5 μ g of Crh1 protein, 18 μ M SR-labeled oligosaccharide (L5-SR or CH5-SR) as the acceptor, and CM-chitin (0.1%) as the donor in 50 mM citrate buffer, pH 4.9. FU, arbitrary fluorescence units. Statistical significance was determined by two-tailed, unpaired, Student's *t*-test compared with no treatment (* $P \leq .05$, ** $P \leq .01$, *** $P \leq .001$; ns, not significant)

assayed Slt2 phosphorylation over time in the presence of a sublethal concentration of PA (100 $\mu\text{g}/\text{mL}$). As shown in Figure 3A, PA induced a rapid increase in the phospho-Slt2 level after 10 minutes and a peak after 1 hour, followed by a decrease until 6 hour.

To confirm the association between PA-induced activation of the CWI pathway and the corresponding cell-wall-related transcriptional response, the expression

profiles of four genes (*MLP1*, *PIR3*, *CWPI*, and *YLR194C*) commonly induced by cell-wall stress and regulated by this pathway²⁶ were analyzed. As shown in Figure 3B, PA induced an increase in the transcript levels of these genes, which peaked after 1 hour and gradually decreased thereafter. Moreover, the induction was dependent on both the MAPK Slt2 and the transcription factor Rlm1 (Figure 4B).

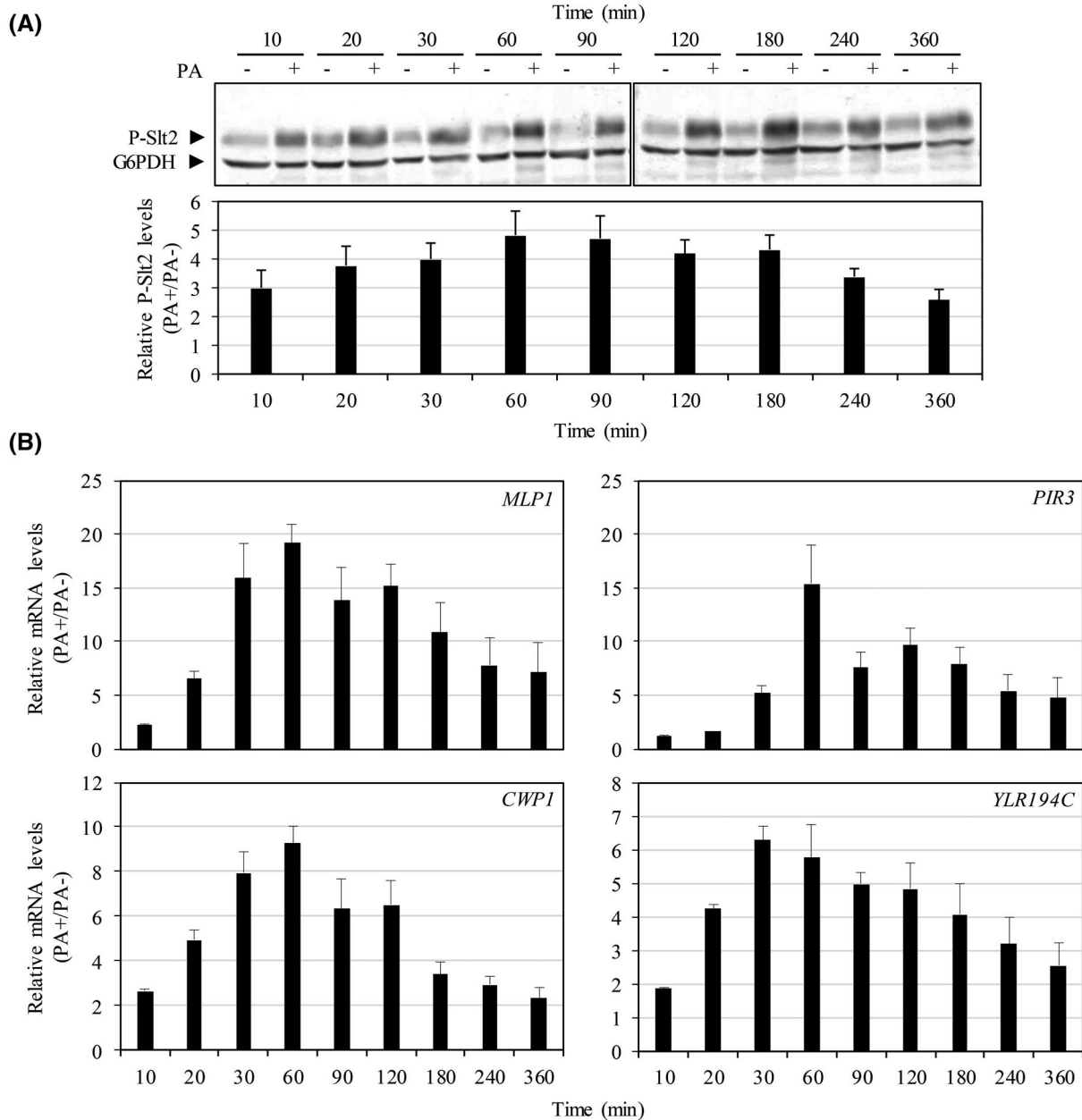


FIGURE 3 Poacic acid (PA) activates the yeast cell-wall integrity (CWI) pathway. A, Time course of Slt2 activation in wild-type (WT) (BY4741) cells cultured at 24°C to mid-logarithmic phase and exposed to PA (100 $\mu\text{g}/\text{mL}$) for the indicated times. Slt2 activation was examined by western blotting total extracts with an anti-phospho-p44/42 mitogen activated protein kinase antibody. Graphs show quantification, by densitometric analysis, of the phospho-Slt2 bands on western blots, normalized to the loading control (G6PDH). Mean values from three independent experiments are shown. B, Expression analysis of the CWI-responsive genes *MLP1*, *PIR3*, *CWPI*, and *YLR194C* by quantitative RT-PCR in WT cells treated or not with PA for the indicated times. Values are PA-treated to nontreated ratios, and data are means and standard deviations of three independent experiments

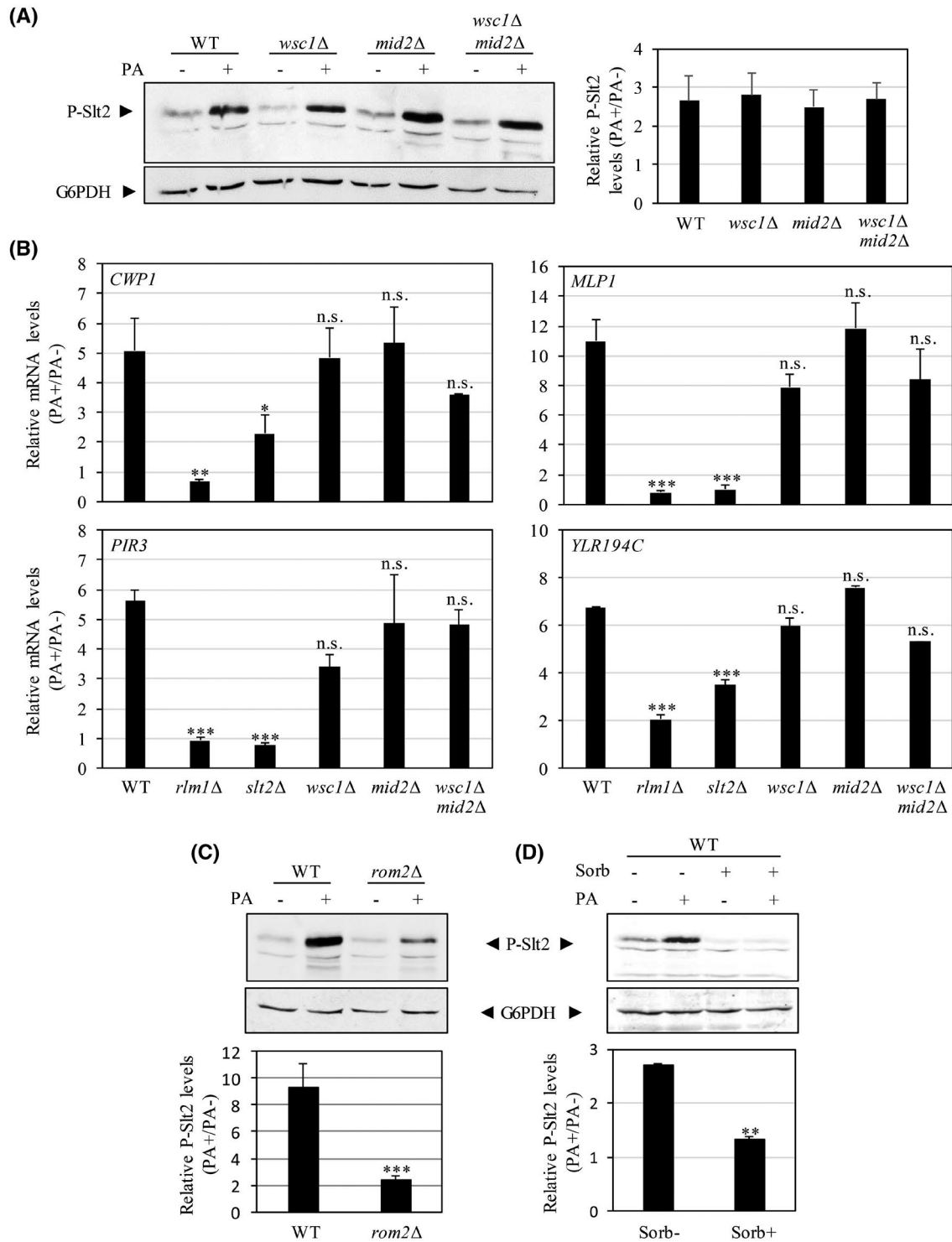


FIGURE 4 Adaptation to poacic acid (PA) requires elements of the cell-wall integrity (CWI) pathway, including the GEF Rom2 but not Mid2 and Wsc1, the main sensors of this pathway. A, Slt2-phosphorylation by PA in *wsc1Δ* (MML282), *mid2Δ* (MML387), and *wsc1Δ mid2Δ* (MML393) strains compared to the wild-type (WT) (CML128). Slt2 activation was examined by western blotting total extracts with an anti-phospho-p44/42 mitogen activated protein kinase antibody using G6PDH as the loading control. B, Expression analysis of the CWI-responsive genes *MLP1*, *PIR3*, *CWP1*, and *YLR194C* by quantitative RT-PCR in the WT and the indicated mutant strains treated or not with PA for 1 hour. Values are PA-treated to nontreated ratios and are means and standard deviations of three independent experiments. C, Phosphorylation of Slt2 by PA (100 μ g/mL, 1 hour) in a *rom2Δ* strain compared with the corresponding WT strain. D, Effect of sorbitol on the phosphorylation of Slt2 by PA in the WT strain. Graphs in (A), (C), and (D) show quantification, by densitometric analysis, of the phospho-Slt2 bands on western blots normalized to the G6PDH band. Mean values from three independent experiments are shown. Statistical significance was determined by two-tailed, unpaired, Student's *t*-test comparing the mutant with the WT strain (* $P \leq .05$, ** $P \leq .01$, *** $P \leq .001$; ns, not significant)

3.5 | Activation of the CWI pathway by PA is not dependent on a single cell-surface sensor

To evaluate the mechanism by which PA activates the CWI pathway, we investigated the five CWI sensors described to date: Wsc1 to Wsc3, Mid2 and Mtl1.^{21,51} We initially investigated the participation of Wsc1 and Mid2 based on their contribution to CWI signaling and partially overlapping functions.^{52,53} As shown in Figure 4A, the level of phospho-Slt2 induced by PA in the WT strain was not decreased in *wsc1Δ* or *mid2Δ* single or a *wsc1Δ mid2Δ* double mutants. Indeed, PA-induced *CWP1*, *MLP1*, *PIR3*, and *YLR194C* expression did not decrease in the single mutants or the double mutant (Figure 4B), suggesting that these sensors do not play an important role in PA signaling or that in their absence other CWI sensors have overlapping functions. Because the activation of Slt2 by caspofungin is blocked in the absence of the sensor Wsc1,^{31,54} our results indicate that the mechanisms of sensing the effect on CWI of PA and caspofungin are different, although both target β -1,3-glucan.

Next, we investigated the effect of deletion of other potential CWI sensors and their combinations to identify those responsible for sensing PA-induced damage. It was impossible to test a full battery of combination mutants because many of the corresponding strains were nonviable. We analyzed the *mtl1Δ mid2Δ*, *mtl1Δ wsc1Δ*, and *mid2Δ wsc2Δ* double mutants and the *wsc1Δ wsc2Δ wsc3Δ* and *mtl1Δ mid2Δ wsc1Δ* triple mutants for Slt2 activation after 1 hour of PA treatment. Strikingly, as shown in Figure S3A, there were no significant differences in phospho-Slt2 levels in these mutants compared to the WT strain. Therefore, PA damage is sensed by an unknown sensor, although the involvement of one or more known CWI sensors cannot be ruled out.

In the absence of the GTP-exchange factor Rom2, which interacts with the cytoplasmic tails of cell-surface sensors to activate the CWI MAPK module, hyperphosphorylation of Slt2 by PA was blocked (Figure 4C), confirming a role for Rom2 in PA-induced signalling. Moreover, bearing in mind the function of the GDP/GTP exchange factor Rom2, which transduce the signal from the cell wall through the CWI sensors to the small GTPase Rho1, triggering the MAPK cascade, it is more likely possible that a cell-surface event rather than a downstream input is responsible for PA-induced MAPK activation. This is reinforced by the fact that in the presence of sorbitol (0.5 M), cells cultured with PA did not show Slt2 hyper-activation (Figure 4D). Supportively, osmotic stabilization of the plasma membrane in the presence of a defective cell wall prevents stimulation of the pathway.⁵⁵

3.6 | The transcriptional response to PA involves genes regulated by the CWI and HOG pathways

To characterize the global transcriptional response elicited by PA in yeast, we carried out RNA-seq using a WT strain grown in the presence or absence of 100 μ g/mL of PA for 1 hour. At this concentration, 137 and 17 genes were significantly twofold up- or down-regulated, respectively (Figure 5A and Table S2). A Gene Ontology (GO) analysis of the PA-upregulated genes revealed significant enrichment of cell-wall biogenesis and remodeling processes, together with morphogenesis, transport, signal transduction, and stress functions (Table S3A). As shown in Figure 5A, the transcriptional response to PA showed marked similarity to global responses to other cell-wall-damage conditions, such as Congo red (chitin-binding dye), zymolyase (enzymatic cocktail including β -1,3-glucanase and chitinase activities), or caspofungin (β -1,3-glucan synthesis inhibitor). Indeed, 49 genes were upregulated by all four conditions (Figure 5B and Table S2), in agreement with the requirement for a common yeast transcriptional reprogramming fingerprint to tolerate cell-wall stress.²⁰ A group of 43 genes was specifically induced by PA and not by the other cell wall-interfering compounds (Figure 5B), although one third of these genes corresponded to genes with no data in the microarray analysis datasheet. Many of the PA-induced genes were of unknown function and genes related to carbohydrate transport and iron chelate transport, including the mannoproteins Fit1 and Fit3, were overrepresented (Table S3B). No significant enrichment of GO terms was found among the 17 genes downregulated by PA, which had a wide variety of functions.

To evaluate the mechanism of action of PA, we investigated the regulatory mechanisms governing its transcriptional response and compared them to those involved in the responses to the other cell-wall-interfering compounds of known mechanisms of action, particularly those targeting β -1,3-glucan. First, we addressed the participation of the MAPK Slt2 by obtaining the genome-wide transcriptional profile of a yeast strain deleted in *SLT2*, grown in the presence of PA for 1 hour. As shown in Figure 5C, of the 137 genes induced by PA in the WT strain, 88 were dependent on Slt2. As expected, most Slt2-dependent genes were functionally related to cell-wall homeostasis (Table S3C), whereas no enrichment in GO biological process terms was found for Slt2-independent genes.

We have recently described a novel connection between the CWI and the PKA pathways that regulates cell wall stress mediated by inhibition of β -1,3-glucan synthesis.³² The global transcriptional response elicited by caspofungin includes a broad group of genes regulated independently of Slt2 corresponding

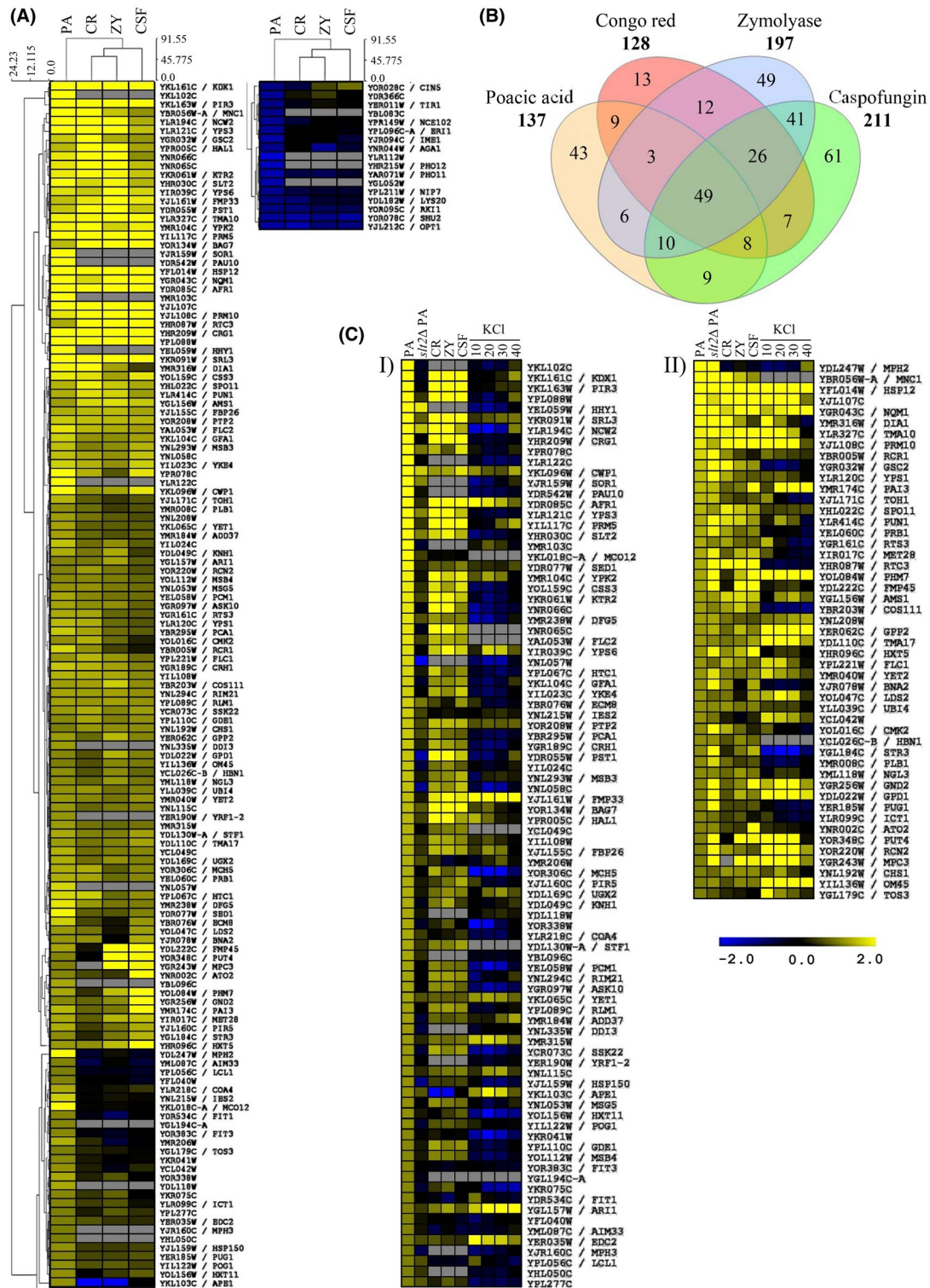


FIGURE 5 Genome-wide expression profiles of the wild-type (BY4741) and *slt2Δ* strains after poacic acid (PA) treatment. A, Hierarchical clustering generated using Multiexperiment Viewer software ver. 4.9 (The Institute for Genomics Research) shows gene expression ratios comparing the transcriptional response of a wild-type strain to PA (100 μg/mL for 1 hour) to other cell-wall stress conditions. Open reading frames whose transcripts were induced (left) or repressed (right) at least twofold by PA are shown and compared to Congo red (CR), zymolyase (ZY) and caspofungin (CSF) genome-wide transcriptional datasets. The degree of color saturation represents the expression log₂ ratio value, as indicated by the scale bar; gray boxes denote missing values. B, Venn diagram of the distribution of yeast genes whose expression was upregulated at least twofold by PA (this work), Congo red, zymolyase, and caspofungin. C, Heat maps of open reading frames whose transcripts were upregulated in an Slit2-dependent (cluster I) or -independent (cluster II) manner by PA are shown and compared to Congo red,²⁶ zymolyase (our unpublished results), caspofungin,³² and KCl⁶³ genome-wide transcriptional datasets

to genes negatively regulated by the cyclic AMP/ PKA signalling pathway. Comparing the PA-Slt2-independent set of genes with those induced by osmotic stress (KCl 0.5 M) or those regulated by the PKA pathway revealed no significant similarity with the PKA responses but includes components of the osmotic stress transcriptional response. Approximately 70% of the genes induced by PA in an Slt2-independent fashion were also induced by KCl (Figure 5C). Therefore, the CWI pathway is the main regulator of the transcriptional response to PA, with participation by the HOG pathway.

3.7 | PA activates the HOG1 MAPK signalling pathway

Having established a link to the HOG MAPK pathway, we analyzed whether Hog1 is activated by PA using antibodies that recognize the phosphorylated form of Hog1. As shown in Figure 6A and similar to zymolyase,²⁷ this MAPK was slightly activated after 1 hour of PA treatment. The PA-induced phosphorylation level of Hog1 was lower than that caused by osmotic stress (such as 0.5 M KCl; Figure 6A), in agreement with the limited osmotic-like transcriptional response identified by RNA-seq. Next, the expression levels of several Slt2-independent osmo-regulated genes were quantified by RT-qPCR in the WT and *hog1Δ* strains. As shown in Figure 6B, *GPD1*, *HSP12*, and *NQM1* were induced by PA in the WT strain in a manner dependent on Hog1 (Figure 6B). Next, we investigated the involvement of the two input branches of the HOG pathway in Hog1-mediated transcriptional activation of these genes by PA. The HOG1 pathway has two branches that activate the MAPK module by different mechanisms. The Sho1 branch requires the mucin-like osmosensors, Hkr1 and Msb2,⁵⁶ whereas the second branch is activated by the transmembrane protein Sln1. As shown in Figure 6B, blocking of either branch by deleting *HKR1* (Sho1 branch) or the redundant *SSK2/SSK22* elements (Sln1 branch) did not affect the transcriptional activation by PA of any of the three genes. However, the induction was completely blocked in an *hkr1Δ ssk2Δ ssk22Δ* triple mutant (Figure 6B), indicating that PA is sensed by the two branches of the pathway. Moreover, the adaptive transcriptional response to zymolyase requires the sequential activation of the HOG and CWI pathways, so Slt2 is not activated in the absence of Hog1. However, this was not so for PA; the P-Slt2 level in the *hog1Δ* strain was similar to that in the WT (Figure 6C). Moreover, elements of the Sho1 and Sln1 branches of the HOG pathway were not required for Slt2 activation by PA (Figure S3B). These results indicate that the transcriptional responses to zymolyase and PA, which affect the cell wall by degrading β-1,3-glucan (zymolyase) or binding to, and interfering

with glucan network maturation (PA), share similar but not identical regulatory mechanisms.

A genome-wide transcriptional analysis of the *slt2Δ* strain revealed that in the absence of *SLT2*, PA included an alternative response with respect to the WT strain (Figure S4). This response involved at least a twofold increase in the expression of 147 genes compared to in the absence of PA, mainly genes related to amino acid and carbohydrate metabolism and osmotic or oxidative stress (Table S3D). Hierarchical clustering of these genes with the genome-wide transcriptional profiles of yeast cells under hyper-osmotic stress conditions revealed a large number of shared genes (Figure S4). This is in agreement with higher activation of Hog1 by PA in the absence of Slt2 (Figure 6A) and the corresponding increased transcript levels of *GPD1*, *HSP12*, and *NQM1* in the *SLT2*-deletion mutant treated with PA compared to the WT (Figure 6B). A similar phenomenon has been reported for zymolyase-mediated stress,²⁸ confirming the mechanism by which the CWI pathway inhibits the HOG pathway under stress conditions.

3.8 | Correlation of sensitivity to PA with β-1,3-glucan content

Our data indicated the CWI pathway to be the main regulator of the transcriptional response to PA, together with the HOG pathway. This is in agreement with a prior report that several genes in the CWI pathway are required for PA resistance.³⁶ The MAPKKK deletion mutant (*bck1Δ*) showed a sixfold reduction in PA IC₅₀ value compared to the WT. Also, the pathway most sensitive to PA was the CWI pathway.³⁶ Information on yeast PA-sensitive mutant strains is important for evaluating the compound's antifungal spectrum. PA inhibits the filamentous growth of a variety of pathogenic fungi, including *S. sclerotiorum* and *A. solani*,³⁶ which have β-1,3-glucan. We also evaluated the PA sensitivity of yeast strains with different β-1,3-glucan contents. Sensitivity to K1 killer toxin is negatively correlated with β-1,6-glucan content because strains with low β-1,6-glucan contents have fewer toxin-binding sites, rendering them resistant.⁵⁷ We next analyzed the PA sensitivity and β-1,3-glucan content of WT yeast isolates; their IC₅₀ values ranged from 244 to >1000 μg/mL (Figure S5A). There was a significant negative correlation between β-1,3-glucan content (Figure S5B) and PA sensitivity (Figure 7A; $R = -0.51$, $P < .01$, Pearson's correlation test). There was a weak positive correlation between echinocandin B sensitivity and β-1,3-glucan content (Figure S6A; $R = 0.40$, $P = .013$, Pearson's correlation test) but no correlation between PA sensitivity and echinocandin B sensitivity (Figure S6B; $R = 0.28$, $P = .096$, Pearson's correlation test), confirming that PA and echinocandin B have different mechanisms of action.

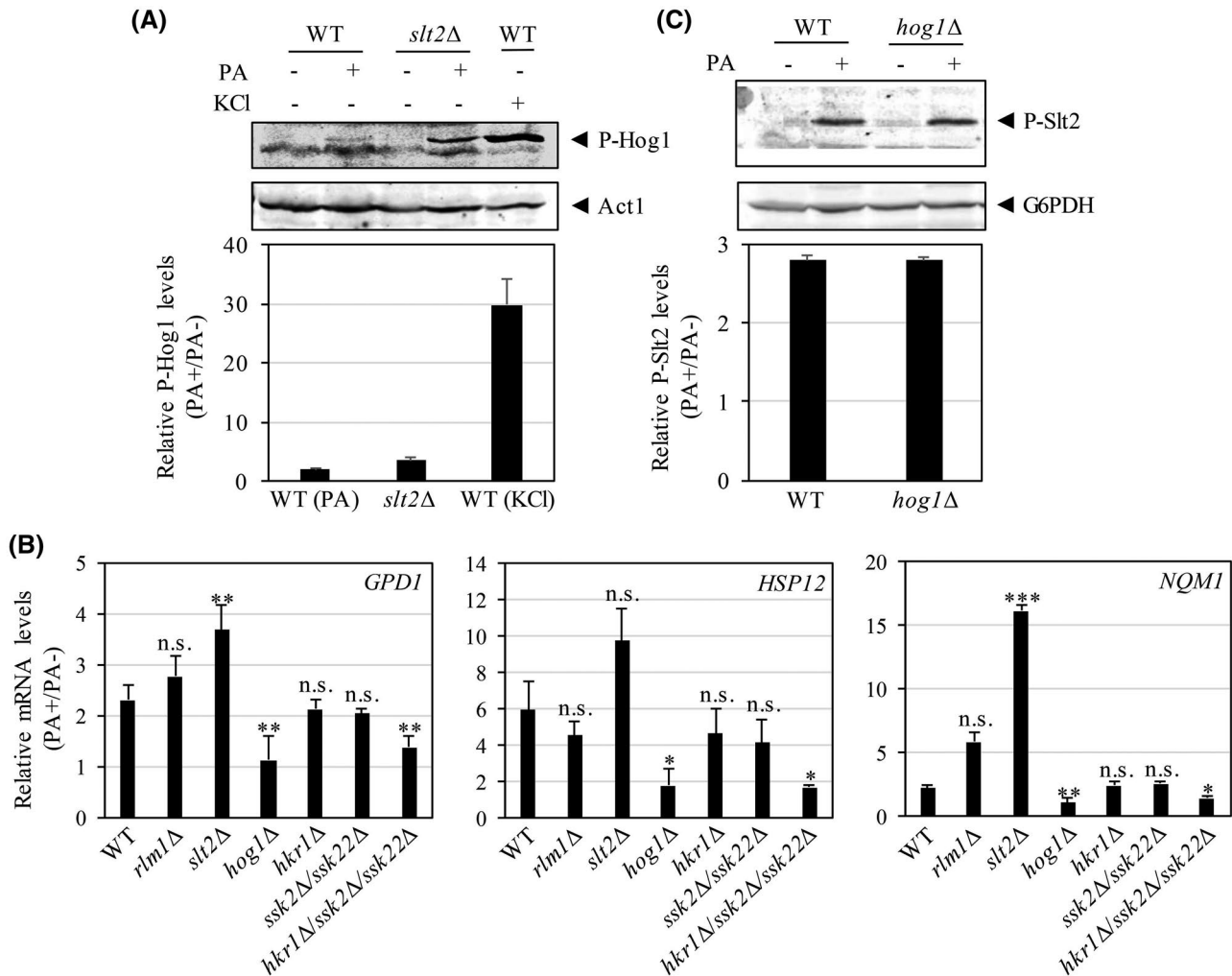


FIGURE 6 Poacic acid (PA) induces an osmotic-like response which is enhanced in the absence of *SLT2*. A, Hog1 is slightly activated by PA in the wild-type (WT) strain and more highly activated in the absence of *SLT2*. Exponentially growing WT and *slt2Δ* cells were collected before and after PA treatment (100 μg/mL, 1 hour), and Hog1 activation was examined by western blotting total extracts with an anti-phospho-p38 antibody. The levels of phosphorylation of Hog1 induced by 0.5 M KCl are also shown. B, Expression analysis of several genes induced by PA in *slt2Δ* but not in the WT. Gene expression was analyzed by quantitative RT-PCR in the WT and the indicated mutant strains treated or not with PA at 1 hour. Values are PA-treated to nontreated ratios and are means and standard deviations of three independent experiments. Statistical significance was determined by two-tailed, unpaired, Student's *t*-test comparing the mutant and WT strains (**P* ≤ .05, ***P* ≤ .01, ****P* ≤ .001; ns, not significant). C, Slt2 phosphorylation by PA is not dependent on Hog1. WT and *hog1Δ* cells were processed as in (A) and Slt2 activation was examined with an anti-phospho-p44/42 mitogen activated protein kinase. Graphics in (A) and (C) show quantification, by densitometric analysis, of the Phospho-Hog1(A) and Phospho-Slt2 (C) bands from the western blot, normalized to the loading control levels of Act1 (A) or G6PDH (C). Mean values from three independent experiments are shown

We assayed the PA sensitivity of temperature-sensitive glucan synthase mutants at 25°C.⁴¹ The mutants exhibited that IC₅₀ ranged values from 27 to 348 μg/mL (Figure S5C). There was a significant negative correlation between β-1,3-glucan content (Figure S5D) and PA sensitivity (Figure 7B; *R* = -0.84, *P* < .01, Pearson's correlation test). There was no correlation between echinocandin B sensitivity and β-1,3-glucan content (Figure S7A; *R* = 0.279, *P* = .41, Pearson's correlation test) or between PA sensitivity and echinocandin B sensitivity (Figure S7B; *R* = 0.364, *P* = .27, Pearson's correlation test). Therefore, PA sensitivity was negatively

correlated with the β-1,3-glucan content of several yeast strains.

4 | DISCUSSION

Our results shed light on the mechanisms by which PA interferes with the β-1,3-glucan network, the transcriptional responses elicited, and the regulatory circuits involved. Direct binding of PA to β-1,3-glucan has been demonstrated qualitatively.³⁶ By quantitatively comparing the binding of PA to

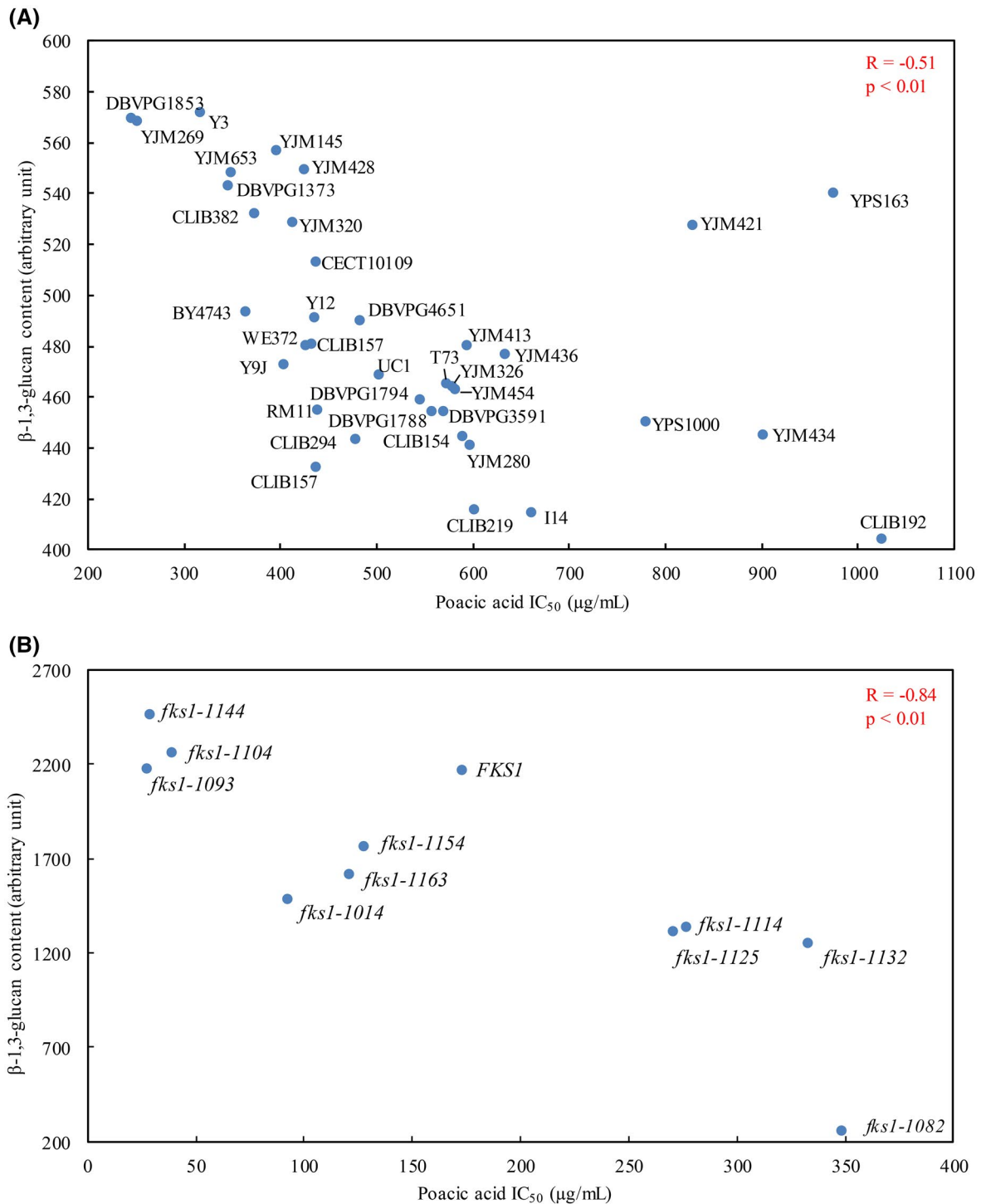


FIGURE 7 β -1,3-Glucan content is negatively correlated with poaic acid (PA) susceptibility in *S. cerevisiae* strains. IC_{50} values of yeast strains after growth in YPD at 25°C for 24 hour in the presence of 15.6, 31.3, 62.5, 125, 250, 500, or 1000 μ g/mL of PA. The β -1,3-glucan content was estimated after growth in YPD and staining with aniline blue (0.5 mg/mL). The fluorescence signal intensity of individual cells was quantified by ImageJ. Correlation of PA susceptibility with β -1,3-glucan content was assessed in *Saccharomyces cerevisiae* natural isolates (A) and *fks1-ts* mutants (B) by calculating Pearson's product-moment correlation (R) with associated *P*-value. Experiments were repeated once more, with similar results

β -1,3-glucan and chitin, we discovered that the primary target of PA in yeast is β -1,3-glucan. Our data, and those published previously, suggest that PA and echinocandins differ in the mechanisms by which they interact with β -1,3-glucan biogenesis. PA binds directly to β -1,3-glucan rather than inhibiting

β -1,3-glucan synthase.^{36,37} Yeasts sense these two effects by different mechanisms, and the regulatory mechanisms of rescue responses via various signaling pathways also differ.

Similar to other cell-wall-perturbing agents—such as Congo red, zymolyase, and caspofungin^{18,20,27,55}—and in

contrast to the rapid and transient osmostress-mediated activation of the MAPK Hog1, PA induces slow and sustained activation of the MAPK Sit2. We show here that the CWI pathway plays an important role in regulating the transcriptional response of *S. cerevisiae* to PA-mediated cell-wall stress. This is in agreement with the fact that strains deleted in elements of this pathway, such as *BCK1* or *ROM2*, confer sensitivity to PA. By contrast, PA does not activate the PKC/Mkc1 cell-wall salvage pathway in *C. albicans*, and deletion of *MKCl* has no impact on PA sensitivity.³⁷ In addition to CWI, other signaling pathways are involved in adaptive transcriptional responses to cell-wall stress. This is the case for the HOG pathway as a consequence of zymolyase treatment²⁸ or the PKA pathway after caspofungin exposure,³² which interfere with glucan biogenesis by degrading the β -1,3-glucan network or inhibiting β -1,3-glucan synthesis, respectively. In the first case, cell-wall damage is sensed by Hkr1 and elements of the Sho1 branch of the HOG pathway, activating a transcriptional adaptive response controlled mainly by Rlm1 that requires sequential activation of the HOG and CWI pathways. By contrast, echinocandins trigger responses sensed by Wsc1, leading to activation of the CWI pathway and parallel inhibition of the PKA signaling pathway.^{20,32} However, PA does not trigger PKA-mediated responses. Additionally, PA induces a transcriptional response involving CWI- and osmotic stress-responsive genes. However, activation of the CWI pathway by PA does not rely on elements of the HOG pathway, suggesting transcriptional co-regulation mediated by parallel activation of both signalling pathways. In contrast to zymolyase, PA signaling via the HOG pathway is transmitted redundantly via the two activation branches reported for this route. Moreover, the GTP-exchange factor Rom2, which interacts with the cytoplasmic tails of cell-surface sensors to activate the CWI MAPK module, is essential for PA-mediated signalling. However, none of the CWI sensors is involved, suggesting that PA-mediated damage is sensed by an as-yet-unknown sensor. Thus, despite sharing β -1,3-glucan as a cellular target, several aspects of the yeast transcriptional responses to echinocandins, zymolyase and PA, particularly those related to the regulatory circuits involved, are different, indicating that their effects on CWI have different mechanisms of action.

Because its activity seems to be mediated by interaction with β -1,3-glucan rather than a direct effect on glucan synthesis, PA likely interferes with β -1,3-glucan maturation. Indeed, the addition of exogenous β -1,3-glucan attenuates PA-mediated inhibition of yeast growth in a dose-dependent manner.³⁷ Linear cell-wall components are synthesized at the plasma membrane and then extruded into the cell-wall space. The final stage of cell-wall construction and remodeling is the creation of covalent cross-links between individual cell-wall components to form a three-dimensional network. β -1,3-glucan chains are elongated and branched by the Gas1-family

BGTs.^{9,11,58} These enzymes split β -1,3-glucan and transfer the newly generated reducing end to the non-reducing end of another β -1,3-glucan molecule or to a branching point created by Bgl2.^{39,59} Additionally, Crh enzymes transglycosylate chitin to β -1,3-glucan and β -1,6-glucan.^{8,12} In vitro, these enzymes also function as homo-transglycosylases to join and elongate chitin chains.³⁹

Using laminarin as donor substrate and SR-labeled laminari-oligosaccharides as acceptors, we demonstrated that PA inhibits the glucanosyltransferase activity of Gas enzymes. We interpret this inhibition as a consequence of the chemical modification of the substrate (β -1,3-glucan and/or the oligosaccharides derived from it), which ultimately would disturb the interaction with the enzyme. Thus, the modified glucans would no longer be a substrate for Gas glucanosyl-transferases.

Moreover, the transglycosylase activity mediated by Crh1 is also inhibited by PA when CM-chitin is used as a donor and β -1,3 oligosaccharides as acceptors, but not when the acceptors are chito-oligosaccharides. Thus, PA targets β -1,3-glucan interfering with the transglycosylation processes. We favor that PA is not interfering directly with the enzymes but interfering with transglycosylation due to its binding to the substrates, both donor and acceptor for the Gas enzymes, and only the acceptor in the case of Crh1. Therefore, our results suggest that binding of PA to glucan would interfere with the maturation processes of β -1,3-glucan, including elongation and branching through Gas Glucanosyltransferases and crosslinking to chitin through Crh proteins. Interference in these processes by PA would ultimately compromise the strength and integrity of the cell wall.

PA, an 8-5 linked dimer of FA, exhibits antifungal activity, but CA and FA have only a slight inhibitory effect on yeast. This suggests that the antifungal action of PA is mediated by a unique aspect of its chemical structure. According to previous studies,^{60,61} the positions and numbers of *trans*-formed double bonds, hydroxy groups, and methoxy groups have a marked effect on phenolic compounds. In particular, functional groups (such as hydroxy and methoxy groups) can be donors or acceptors of hydrogen bonds. Because these functional groups could act efficiently on β -1,3-glucan, the stereochemistry of the *trans*-formed double bond is important.^{60,61}

Our current understanding is that at least three factors affect PA antifungal activity. The first one is the level of β -1,3-glucan in the fungal cell wall. In natural and *fks-ts* mutant strains of *S. cerevisiae*, we found a significant negative correlation between β -1,3-glucan content and PA susceptibility. This suggested that the β -1,3-glucan content affects the antifungal activity spectrum of PA. This is consistent with the fact that PA was effective for *S. sclerotiorum*, which has highly polymerized β -1,3-glucan.^{36,62} The second one is the activity of the CWI pathway. Yeast mutants defective

in the CWI pathway exhibited PA susceptibility but had an unchanged β -1,3-glucan content.³⁶ This would suggest that the fungal species with the activated CWI pathway result in PA resistance. The third one is the topology of Fks1 on the plasma membrane.³⁷ In contrast to *S. cerevisiae*, there was no correlation between the β -1,3-glucan content and PA susceptibility of *Candida* species.³⁷ Instead, the membrane topology of Fks1 is related to PA susceptibility of *Candida* species. Thus, the β -1,3-glucan content and other factors likely determine the antifungal activity spectrum of PA.

DATA AVAILABILITY STATEMENT

The RNA-seq data follow the recommendations for the minimum required information about a high-throughput sequence and have been deposited at the National Center for Biotechnology Information gene expression and hybridization array and sequence-based data repository under accession number GSE165530.

ACKNOWLEDGMENTS

We sincerely thank Fachuang Lu, Ruili Gao, Jeff Piotrowski, and John Ralph for providing poacic acid and Kozo Tomita for permission to use a spectrophotometer. We want to thank Jesús García-Cantalejo, Pedro Botías, and Rosa Pérez at the Genomics Unit (UCM) for their help with the RT-qPCR and genome-wide expression analysis. We are in debt with Francesc Posas, María Angeles de la Torre, Haruo Saito, Francisca Rández, and Katrina F. Cooper for providing strains. We are particularly in debt with Vladimír Farkaš for the synthesis of fluorescence-labelled oligosaccharides for the enzymatic assays. All members of our research group (UCM-920640: Yeast Functional Genomics) at the Department of Microbiology and Parasitology (UCM) are also acknowledged for their support.

CONFLICT OF INTEREST

The authors do not declare any conflict of interest.

AUTHOR CONTRIBUTIONS

J. Arroyo and Y. Ohya conceived the study and designed experiments. R. García, K. Itto-Nakama, J.M. Rodríguez-Peña, A.B Sanz, X. Chen, A. de Lorenzo, and M. Pavón-Vergés performed experiments and interpreted results. L. Popolo produced recombinant proteins. C. Nombela analyzed data. K. Kubo and S. Ohnuki supported students. J. Arroyo, Y. Ohya, and J.M. Rodríguez-Peña wrote the manuscript and analyzed data. R. García and K. Itto-Nakama designed the figures.

ORCID

Javier Arroyo  <https://orcid.org/0000-0002-1971-1721>

REFERENCES

- Bongomin F, Gago S, Oladele RO, Denning DW. Global and multi-national prevalence of fungal diseases-estimate precision. *J Fungi*. 2017;3(4):1-29.
- Wiederhold NP. The antifungal arsenal: alternative drugs and future targets. *Int J Antimicrob Agents*. 2018;51(3):333-339.
- Cortés JCG, Curto MA, Carvalho VSD, Pérez P, Ribas JC. The fungal cell wall as a target for the development of new antifungal therapies. *Biotechnol Adv*. 2019;37(6). 107352.
- Tada R, Latgé JP, Aïmanianda V. Undressing the fungal cell wall/cell membrane—the antifungal drug targets. *Curr Pharm Des*. 2013;19(20):3738-3747.
- Gow NAR, Latgé JP, Munro CA. The fungal cell wall: structure, biosynthesis, and function. *Microbiol Spectr*. 2017;5(3):1-25.
- Orlean P. Architecture and biosynthesis of the *Saccharomyces cerevisiae* cell wall. *Genetics*. 2012;192(3):775-818. <https://doi.org/10.1534/genetics.1112.144485>
- Free SJ. Fungal cell wall organization and biosynthesis. *Adv Genet*. 2013;81:33-82.
- Cabib E, Arroyo J. How carbohydrates sculpt cells: chemical control of morphogenesis in the yeast cell wall. *Nat Rev Microbiol*. 2013;11(9):648-655.
- Mouyna I, Fontaine T, Vai M, et al. Glycosylphosphatidylinositol-anchored glucanoyltransferases play an active role in the biosynthesis of the fungal cell wall. *J Biol Chem*. 2000;275(20):14882-14889.
- Mazán M, Ragni E, Popolo L, Farkaš V. Catalytic properties of the Gas family beta-(1,3)-glucanoyltransferases active in fungal cell-wall biogenesis as determined by a novel fluorescent assay. *Biochem J*. 2011;438(2):275-282.
- Aïmanianda V, Simenel C, Garnaud C, et al. The dual activity responsible for the elongation and branching of beta-(1,3)-glucan in the fungal cell wall. *mBio*. 2017;8(3):1-14.
- Arroyo J, Farkaš V, Sanz AB, Cabib E. Strengthening the fungal cell wall through chitin-glucan cross-links: effects on morphogenesis and cell integrity. *Cell Microbiol*. 2016;18(9):1239-1250.
- Cabib E. Two novel techniques for determination of polysaccharide cross-links show that Crh1p and Crh2p attach chitin to both beta(1-6)- and beta(1-3)glucan in the *Saccharomyces cerevisiae* cell wall. *Eukaryot Cell*. 2009;8(11):1626-1636.
- Cabib E, Blanco N, Grau C, Rodríguez-Peña JM, Arroyo J. Crh1p and Crh2p are required for the cross-linking of chitin to beta(1-6) glucan in the *Saccharomyces cerevisiae* cell wall. *Mol Microbiol*. 2007;63(3):921-935.
- Rodríguez-Peña JM, Cid VJ, Arroyo J, Nombela C. A novel family of cell wall-related proteins regulated differently during the yeast life cycle. *Mol Cell Biol*. 2000;20(9):3245-3255.
- Levin DE. Regulation of cell wall biogenesis in *Saccharomyces cerevisiae*: the cell wall integrity signaling pathway. *Genetics*. 2011;189(4):1145-1175.
- Popolo L, Gualtieri T, Ragni E. The yeast cell-wall salvage pathway. *Med Mycol*. 2001;39(suppl 1):111-121.
- García R, Bermejo C, Grau C, et al. The global transcriptional response to transient cell wall damage in *Saccharomyces cerevisiae* and its regulation by the cell integrity signaling pathway. *J Biol Chem*. 2004;279(15):15183-15195.
- Lagorce A, Hauser NC, Labourdette D, et al. Genome-wide analysis of the response to cell wall mutations in the yeast *Saccharomyces cerevisiae*. *J Biol Chem*. 2003;278(22):20345-20357.

20. Sanz AB, García R, Rodríguez-Peña JM, Arroyo J. The CWI pathway: regulation of the transcriptional adaptive response to cell wall stress in yeast. *J Fungi*. 2017;4(1):1-12.
21. Kock C, Dufrene YF, Heinisch JJ. Up against the wall: is yeast cell wall integrity ensured by mechanosensing in plasma membrane microdomains? *Appl Environ Microbiol*. 2015;81(3):806-811.
22. Elhasi T, Blomberg A. Integrins in disguise – mechanosensors in *Saccharomyces cerevisiae* as functional integrin analogues. *Microb Cell*. 2019;6(8):335-355.
23. Heinisch JJ, Rodicio R. Protein kinase C in fungi—more than just cell wall integrity. *FEMS Microbiol Rev*. 2018;42(1):22-39.
24. García R, Sanz AB, Rodríguez-Peña JM, Nombela C, Arroyo J. Rlm1 mediates positive autoregulatory transcriptional feedback that is essential for Slt2-dependent gene expression. *J Cell Sci*. 2016;129(8):1649-1660.
25. Arroyo J, Bermejo C, García R, Rodríguez-Peña JM. Genomics in the detection of damage in microbial systems: cell wall stress in yeast. *Clin Microbiol Infect*. 2009;15(suppl 1):44-46.
26. Sanz AB, García R, Rodríguez-Peña JM, et al. Chromatin remodeling by the SWI/SNF complex is essential for transcription mediated by the yeast cell wall integrity MAPK pathway. *Mol Biol Cell*. 2012;23(14):2805-2817.
27. Bermejo C, Rodríguez E, García R, et al. The sequential activation of the yeast HOG and SLT2 pathways is required for cell survival to cell wall stress. *Mol Biol Cell*. 2008;19(3):1113-1124.
28. García R, Rodríguez-Peña JM, Bermejo C, Nombela C, Arroyo J. The high osmotic response and cell wall integrity pathways cooperate to regulate transcriptional responses to zymolyase-induced cell wall stress in *Saccharomyces cerevisiae*. *J Biol Chem*. 2009;284(16):10901-10911.
29. Rodríguez-Peña JM, Díez-Muñiz S, Bermejo C, Nombela C, Arroyo J. Activation of the yeast cell wall integrity MAPK pathway by zymolyase depends on protease and glucanase activities and requires the mucin-like protein Hkr1 but not Msb2. *FEBS Lett*. 2013;587(22):3675-3680.
30. Udom N, Chansongkrow P, Charoensawan V, Auesukaree C. Coordination of the cell wall integrity and high-osmolarity glycerol pathways in response to ethanol stress in *Saccharomyces cerevisiae*. *Appl Environ Microbiol*. 2019;85(15):1-16.
31. Reinoso-Martin C, Schuller C, Schuetzer-Muehlbauer M, Kuchler K. The yeast protein kinase C cell integrity pathway mediates tolerance to the antifungal drug caspofungin through activation of Slt2p mitogen-activated protein kinase signaling. *Eukaryot Cell*. 2003;2(6):1200-1210.
32. García R, Bravo E, Díez-Muñiz S, Nombela C, Rodríguez-Peña JM, Arroyo J. A novel connection between the cell wall integrity and the PKA pathways regulates cell wall stress response in yeast. *Sci Rep*. 2017;7(1):5703.
33. Denning DW, Bromley MJ. Infectious disease. How to bolster the antifungal pipeline. *Science*. 2015;347(6229):1414-1416.
34. Perfect JR. The antifungal pipeline: a reality check. *Nat Rev Drug Discov*. 2017;16(9):603-616.
35. Nett JE, Andes DR. Antifungal agents: spectrum of activity, pharmacology, and clinical indications. *Infect Dis Clin North Am*. 2016;30(1):51-83.
36. Piotrowski JS, Okada H, Lu F, et al. Plant-derived antifungal agent poaic acid targets beta-1,3-glucan. *PNAS*. 2015;112(12):E1490-E1497.
37. Lee KK, Kubo K, Abdelaziz JA, et al. Yeast species-specific, differential inhibition of beta-1,3-glucan synthesis by poaic acid and caspofungin. *Cell Surf*. 2018;3:12-25.
38. Livak KJ, Schmittgen TD. Analysis of relative gene expression data using real-time quantitative PCR and the 2(-Delta Delta C(T)) method. *Methods*. 2001;25(4):402-408.
39. Mazán M, Blanco N, Kováčová K, et al. A novel fluorescence assay and catalytic properties of Crh1 and Crh2 yeast cell wall transglycosylases. *Biochem J*. 2013;455(3):307-318.
40. Yvert G, Ohnuki S, Nogami S, et al. Single-cell phenomics reveals intra-species variation of phenotypic noise in yeast. *BMC Syst Biol*. 2013;7:54.
41. Okada H, Abe M, Asakawa-Minemura M, et al. Multiple functional domains of the yeast 1,3-beta-glucan synthase subunit Fks1p revealed by quantitative phenotypic analysis of temperature-sensitive mutants. *Genetics*. 2010;184(4):1013-1024.
42. Okada H, Ohya Y. Fluorescent labeling of yeast cell wall components. *Cold Spring Harb Protoc*. 2016;2016(8):699-702.
43. Evans NA, Hoynes PA, Stone BA. Characteristics and specificity of the interaction of a fluorochrome from aniline blue (sirofluor) with polysaccharides. *Carbohydr Polym*. 1984;4(3):215-230.
44. Beauvais A, Bruneau JM, Mol PC, Buitrago MJ, Legrand R, Latgé JP. Glucan synthase complex of *Aspergillus fumigatus*. *J Bacteriol*. 2001;183(7):2273-2279.
45. Walker LA, Munro CA, de Bruijn I, Lenardon MD, McKinnon A, Gow NA. Stimulation of chitin synthesis rescues *Candida albicans* from echinocandins. *PLoS Pathog*. 2008;4(4):e1000040.
46. Ram AF, Klis FM. Identification of fungal cell wall mutants using susceptibility assays based on calcofluor white and Congo red. *Nat Protoc*. 2006;1(5):2253-2256.
47. Costa-de-Oliveira S, Silva AP, Miranda IM, et al. Determination of chitin content in fungal cell wall: an alternative flow cytometric method. *Cytometry A*. 2013;83(3):324-328.
48. Shedletzky E, Unger C, Delmer DP. A microtiter-based fluorescence assay for (1,3)-beta-glucan synthases. *Anal Biochem*. 1997;249(1):88-93.
49. Fernandes C, Anjos J, Walker LA, et al. Modulation of *Alternaria infectoria* cell wall chitin and glucan synthesis by cell wall synthase inhibitors. *Antimicrob Agents Chemother*. 2014;58(5):2894-2904.
50. Lee HS, Kim Y. *Aucklandia lappa* causes cell wall damage in *Candida albicans* by reducing chitin and (1,3)-beta-D-glucan. *J Microbiol Biotechnol*. 2020;30(7):967-973.
51. Kock C, Arlt H, Ungermann C, Heinisch JJ. Yeast cell wall integrity sensors form specific plasma membrane microdomains important for signalling. *Cell Microbiol*. 2016;18(9):1251-1267.
52. Jendretzki A, Wittland J, Wilk S, Straede A, Heinisch JJ. How do I begin? Sensing extracellular stress to maintain yeast cell wall integrity. *Eur J Cell Biol*. 2011;90(9):740-744.
53. Levin DE. Cell wall integrity signaling in *Saccharomyces cerevisiae*. *Microbiol Mol Biol Rev*. 2005;69(2):262-291.
54. Bermejo C, García R, Straede A, et al. Characterization of sensor-specific stress response by transcriptional profiling of wsc1 and mid2 deletion strains and chimeric sensors in *Saccharomyces cerevisiae*. *OMICS*. 2010;14(6):679-688.
55. de Nobel H, Ruiz C, Martin H, et al. Cell wall perturbation in yeast results in dual phosphorylation of the Slt2/Mpk1 MAP kinase and in an Slt2-mediated increase in FKS2-lacZ expression, glucanase resistance and thermotolerance. *Microbiology*. 2000;146(pt 9):2121-2132.

56. Tatebayashi K, Tanaka K, Yang H-Y, et al. Transmembrane mucins Hkr1 and Msb2 are putative osmosensors in the SHO1 branch of yeast HOG pathway. *EMBO J.* 2007;26(15):3521-3533.
57. Brown JL, Kossaczka Z, Jiang B, Bussey H. A mutational analysis of killer toxin resistance in *Saccharomyces cerevisiae* identifies new genes involved in cell wall (1→6)-beta-glucan synthesis. *Genetics.* 1993;133(4):837-849.
58. Latgé JP. 30 years of battling the cell wall. *Med Mycol.* 2017;55(1):4-9.
59. Mouyna I, Monod M, Fontaine T, Henrissat B, Lechenne B, Latgé JP. Identification of the catalytic residues of the first family of beta(1-3)glucanosyltransferases identified in fungi. *Biochem J.* 2000;347(pt 3):741-747.
60. Chen J, Yang J, Ma L, Li J, Shahzad N, Kim CK. Structure-antioxidant activity relationship of methoxy, phenolic hydroxyl, and carboxylic acid groups of phenolic acids. *Sci Rep.* 2020;10(1):2611.
61. Sánchez-Maldonado AF, Schieber A, Ganzle MG. Structure-function relationships of the antibacterial activity of phenolic acids and their metabolism by lactic acid bacteria. *J Appl Microbiol.* 2011;111(5):1176-1184.
62. Ohno N, Suzuki I, Yadomae T. Structure and antitumor activity of a beta-1,3-glucan isolated from the culture filtrate of *Sclerotinia sclerotiorum* IFO 9395. *Chem Pharm Bull (Tokyo).* 1986;34(3):1362-1365.
63. O'Rourke SM, Herskowitz I. Unique and redundant roles for HOG MAPK pathway components as revealed by whole-genome expression analysis. *Mol Biol Cell.* 2004;15(2):532-542.

SUPPORTING INFORMATION

Additional Supporting Information may be found online in the Supporting Information section.

How to cite this article: García R, Itto-Nakama K, Rodríguez-Peña JM, et al. Poacic acid, a β -1,3-glucan-binding antifungal agent, inhibits cell-wall remodeling and activates transcriptional responses regulated by the cell-wall integrity and high-osmolarity glycerol pathways in yeast. *FASEB J.* 2021;35:e21778. <https://doi.org/10.1096/fj.202100278R>